Photodegradation of Bitumen-Derived Organics in Oil Sands Process-Affected Water

Jonathan K. Challis, Angelique Parajas, Julie C. Anderson, Evelyn Asiedu, Jonathan W. Martin, Charles S. Wong, and Matthew S. Ross

Photodegradation of Bitumen-Derived Organics in Oil Sands Process-Affected Water

Jonathan K. Challis[1,2§], Angelique Parajas[1], Julie Anderson[1], Evelyn Asiedu[3], Jonathan W. Martin[4], Charles S. Wong[1,5,6], Matthew S Ross[7*]

[1] Department of Chemistry, Richardson College for the Environment, The University of Winnipeg, Winnipeg, MB R3B 2E9

[2] Department of Chemistry, University of Manitoba, Winnipeg, MB R3T 2N2

[3] Department of Laboratory Medicine and Pathology, Faculty of Medicine and Dentistry, University of Alberta, Edmonton, AB T6G 2R7

[4] Department of Environmental Science and Analytical Chemistry, Stockholm University, Stockholm, Sweden

[5]School of Environment, Jinan University, Guangzhou 510632 China

[6]Southern California Coastal Water Research Project Authority, Costa Mesa CA 92626

[7]Department of Physical Sciences, MacEwan University, Edmonton, AB T5J 2P2

[§]current affiliation: Toxicology Centre, University of Saskatchewan, Saskatoon, SK S7N 5B3

*Corresponding author – Email: rossm48@macewan.ca

Abstract

The chemical composition of water-soluble organics in oil sands process-affected water (OSPW) is primarily composed of natural constituents of bitumen that are solubilized and concentrated during aqueous extraction of oil sands. OSPW organics are persistent and acutely toxic, and a leading remediation strategy is long-term ageing in end-pit lakes, despite limited data available on its photochemical fate. Here, direct photolysis of whole OSPW, or of its constituent fractions, was examined at environmentally relevant wavelengths (>290 nm) in bench-top studies. Changes in the chemical profiles of whole OSPW, acid- (AEO), and base-extractable organics (BEO) were characterized by liquid chromatography with ultra-high resolution mass spectrometry in negative (-) and positive (+) ionization modes. Following 18 d of irradiation, photolysis reduced the total ion intensity in all samples in both modes. The most photo-labile species included the O_2^-, O_3^-, O_4^-, O_2S^-, and O_4S^- chemical classes, which were depleted in whole OSPW by 93-100% after only 5 d. In positive mode, detected species were more recalcitrant than those detected in negative mode, with an average reduction across all heteroatomic classes of 75 ± 11.0% after 18d. Estimated environmental half-lives for heteroatomic classes ranged from 57 d (O_4S^-) to 545 d (O_3N^+), with a greater recalcitrance for classes detected in positive mode compared to negative mode. Under field conditions in end-pit lakes, natural photolysis may be an important mechanism for effective OSPW remediation, and we suggest that future end-pit lakes be shallow to maximize light penetration and natural photolysis in ageing OSPW.

Environmental Significance Statement

Large quantities of oil sands process-affected water (OSPW), produced as a result of the bitumen extraction process of surface mined oil sands, are temporarily stored in large tailings ponds during active mining. A primary strategy for remediation of the dissolved toxic and persistent organics in OSPW is long-term storage in end-pit lakes, despite that little data are available on their photolytic fate. This study demonstrates that photodegradation of known toxic chemical classes occurs on the time scale of months to years and is a potentially important pathway for the removal or transformation of dissolved organics in OSPW. These findings have implications for the treatment, detoxification, and reclamation of OSPW in the many end-pit lakes planned in Northern Alberta. Our results may also be more broadly applicable to the remediation of other petroleum contaminated waters, as similar chemicals as those investigated here are formed through refining or environmental degradation of petroleum.

Table of Contents Art

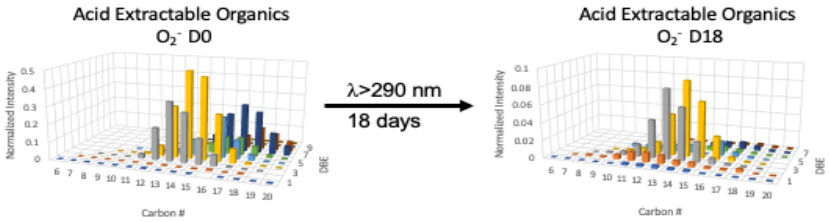

Photolysis results in degradation of known toxic components of oil sands process-affected water (OSPW).

1. Introduction

The production of bitumen from surface-mined oil sands deposits in Northern Alberta requires 2.5 to 4 barrels of water for every barrel of oil produced.[1] The water that has been used in the extraction process is termed oil sands process-affected water (OSPW). This OSPW may have toxicity towards aquatic organisms and is stored on-site in large tailings ponds until remediated, as the industry currently operates under a zero-discharge practice. It is estimated that 720 million m^3 of OSPW are currently stored in tailings ponds,[2] and these volumes are expected to increase with further expansion of the surface-mining industry.

Studies aimed at understanding the chemical composition and toxicity of OSPW have, in the past, focused primarily on naphthenic acids (NAs) —a complex mixture of carboxylic acids naturally formed through the biodegradation of petroleum. NAs can be comprised of acyclic, aromatic, or cyclo-aliphatic species, with varying degrees of cyclization, saturation, and alkyl-substitution. They are described by the general formula $C_nH_{2n+z}O_2$, where z is zero or an even, negative integer indicating the hydrogen deficiency brought about by rings or double bonds.[3,4] Toxicity of OSPW towards aquatic and terrestrial biota has been largely attributed to NAs and NA-like compounds.[5–8] In recent years, however, the application of ultra-high resolution mass spectrometry[9] and multi-dimensional chromatography[10–12] has revealed that the chemical composition of water soluble organics in OSPW is incredibly complex and includes a multitude of other compound classes in addition to NAs. These classes include oxidized NAs,[13] sulfur- and nitrogen-containing acids,[14,15] organic bases,[16] and a diverse array of polar non-acid neutral species.[9,17] Like NAs, these compounds are natural constituents of bitumen and become solubilized and concentrated in OSPW during extraction of bitumen from oil sands ore.[18]

Dissolved organic contaminants undergo biotic and abiotic transformation processes that reduce their concentrations in the environment, resulting in changes to the chemical profiles of complex mixtures. Previous work has revealed differences in the profiles of NAs between bitumen influenced by groundwater and those present in the Athabasca river, leading to the hypothesis that abiotic transformation processes, and in particular, photolysis, altered the chemical profiles of NAs in the environment.[19] As well, temporal trends in the NA profile of OSPW suggests alterations by natural processes.[20,21] Comparisons of compound class profiles generated using high- and ultra-high resolution mass spectrometry have been used to

differentiate natural bitumen-produced organic species from those that have been impacted by the bitumen extraction processes.[21–26] Chemical profiles are used to help determine potential sources of NAs and other bitumen-derived organics in surface waters;[19,24,26,27] however, it is well known that weathering processes, such as biodegradation and photolysis, alter the distribution of chemical species in spilled petroleum and that an understanding and accounting of these factors is required for accurate source determination.[28] Therefore, for chemical profiling to be applicable for the source identification of NAs and other bitumen-derived organics, a greater understanding of how environmental fate processes alter chemical fingerprints is required.

Biotic transformation processes (i.e., biodegradation) of bitumen-derived compounds, including NAs and NA-like organic acids, have been well-studied, and data on structure-activity relationships, kinetics, and pathways are available.[29] Abiotic transformation processes (e.g., photolysis, hydrolysis) of NA-like organic acids, however, remain understudied. Direct and indirect photolysis are significant removal mechanisms for many environmental pollutants, and may represent a potentially important transformation pathway for NAs and other bitumen-derived organic species in OSPW and surface waters.[30] Photodegradation studies have investigated the use of TiO_2 catalysts[15,31–33] or UV-C light (λ<290 nm)[34] to actively degrade NAs and target more recalcitrant species for purposes of remediation. Compositional changes, wherein concentrations of higher molecular weight compounds decreased and concentrations of lower molecular weight compounds concomitantly increased, along with an increase in the proportion of more oxygenated species, were observed following irradiation of OSPW-derived NAs by UV light (λ=254 nm).[18,35]

Natural remediation of OSPW in man-made settling ponds (known as “end pit lakes”) has been proposed as a long-term approach to remediation.[2,5,36] However, few studies have investigated environmentally-relevant (λ>290 nm) photochemical transformation of organic species from OSPW.[3] Given the high turbidity in tailings ponds, photolysis of NAs has been thought to be limited to very near-surface depths where sunlight can penetrate (~1 mm).[35] However, in less turbid surface waters, where sunlight penetration may typically still be relevant to 5-10 cm depths,[37] photolysis may be responsible for alterations in the chemical profiles observed between groundwater and surface waters.[19] Although saturated carboxylic acids are resistant to direct photodegradation,[35] some NA-like organic acids are aromatic[10,38] and absorb photons in the UV-A and UV-B ranges.[39] In addition, observed compositional changes of NAs in

OSPW has indicated t.he presence of a photolabile fraction,[35] suggesting further exploration of photodegradation under environmentally-relevant conditions is warranted.

The present study investigates the effect of simulated natural photodegradation on bitumen-derived dissolved organic species present in OSPW, as well as the isolated acid extractable and base extractable species in OSPW, using ultra-high resolution Orbitrap mass spectrometry. Analyses were conducted in both positive and negative ion atmospheric pressure chemical ionization (APCI) modes, providing a holistic picture of compositional changes. We hypothesized that organic compounds with greater numbers of double bond equivalents (DBE; indicative of increased double bonds, rings, and aromaticity) are more susceptible to photochemical transformation and that this process may be a significant removal pathway for these species in the environment. The current study was intended to provide greater insight regarding the extent to which natural photolysis could be changing the composition of bitumen-derived organic species profiles in the environment.

2. Experimental

2.1. Chemicals and reagents

OSPW was collected from the Mildred Lake Settling Basin (Syncrude Canada, Ltd.) and shipped in 5-gallon polyethylene buckets. Upon arrival, 1-L subsamples were aliquoted into polyethylene bottles and frozen until use.

Methanol and acetonitrile were of HPLC grade (Fisher Scientific) and all water was ultrapure and produced in-house by reverse osmosis (>18 MΩ-cm, Milli-Q RG, Millipore Corp., Ann Arbor, MI). Acetic acid (95%; Sigma–Aldrich, St. Louis, MO) was used for pH buffering during HPLC analysis. Immediately prior to analysis, all samples were spiked with 100 µL of a solution containing 10 mg/L of d_{23}-lauric acid (CDN Isotopes, Pointe-Claire, QC) as an internal standard for negative mode analyses. No internal standard was added for positive mode analyses.

2.2. Preparation of test solutions

Prior to the photolysis experiments, OSPW and reverse osmosis water blanks were sequentially filtered through 6 µm and 2.5 µm Whatman cellulose qualitative filters. This filtered OSPW was further filtered (twice) through 0.45 µm Supelco® nylon filters to produce the first experimental solution, referred to as “whole OSPW”. The other experimental solutions are

referred to as the "acid-extractable organic" (AEO) and "base-extractable organic" (BEO) samples. The AEO samples were prepared from OSPW using an adaptation of an acid fraction extraction method.[40] Briefly, 100 mL aliquots of whole OSPW were added to individual Erlenmeyer flasks and acidified to pH <2 with 1 M H_2SO_4 (99.999%; Sigma–Aldrich, St. Louis, MO). These were extracted by reverse phase solid phase extraction (SPE) using Isolute ENV+ SPE cartridges (200 mg, Biotage, Charlotte, NC), which contain a crosslinked hydroxylated polystyrene-divinylbenzene copolymer stationary phase and which generally retains neutral polar and non-polar analytes. Cartridges were conditioned with 10 mL of methanol followed by 10 mL of water. Aliquots were loaded onto cartridges at a rate of ~5 mL/min and allowed to dry for 30 min. The sorbed organics were eluted with 10 mL of methanol into pre-weighed vials, evaporated to dryness with N_2, and re-weighed.

The BEO samples were also prepared from whole OSPW, but the pH of whole OSPW (100 mL aliquots) was increased to 11 with NH_4OH (reagent grade, Sigma–Aldrich) and similarly extracted by SPE using Isolute ENV+ cartridges. The SPE cartridges were conditioned and washed with 10 mL of 1% (vol/vol) NH_4OH in water and loaded at a rate of ~5 mL/min. After drying for 30 min, the sorbed organics were eluted with 10 mL of methanol into pre-weighed vials, evaporated to dryness with N_2, and re-weighed. The whole OSPW, and dry AEO and BEO samples were stored at 4°C in the dark until their use in photolysis experiments.

2.3. Photolysis experiments

A Rayonet Merry-Go-Round Photochemical Reactor (Figure S1) equipped with 16 medium-pressure mercury lamps (spectral emission 250 – 400 nm, centered at 300 nm) was used for all irradiations (model RPR-100, The Southern New England Ultraviolet Company, Branford, CT). The spectral emission profile of these lamps can be found elsewhere. [37,41] Cylindrical Pyrex tubes (50 mL) that filtered wavelengths of <290 nm were used as irradiation vessels. The average photon flux of the photoreactor was measured in previous studies using chemical actinometry, and ranged from 1.0 to 1.6 ($\times 10^{15}$ photons cm^{-2} s^{-1}). [37,41] This is approximately 50 times more intense than natural sunlight at 50 ˚N latitude (i.e., at a latitude comparable to that of the Alberta oil sands) over the same wavelength range (≈290-360 nm).[42]

Dried AEO (0.0132 g) and BEO (0.0129 g) samples were dissolved in 250 mL of 10 mM NaOH (pH=11.3) and 10 mM HCl (pH=2.4), respectively, to make AEO and BEO solutions of approximately 50 mg/L. Irradiations were conducted over 18 d with 25 mL of solution in each Pyrex tube. Triplicate AEO and BEO samples were exposed in the photoreactor simultaneously and sub-sampled (1.5 mL) into 2 mL amber liquid chromatography vials at 0, 5, 10, and 18 d. Two control experiments (Dark and Dark Kill) experiments were carried out concurrently in a dark oven matching the maximal temperature reached in the photoreactor over the exposure duration (45 – 47 ˚C). Dark exposures were designed to account for non-photolytic abiotic degradation (e.g., hydrolysis, thermal degradation) and microbial transformation. Dark Kill samples were spiked at 10 mM with $HgCl_2$ and were designed to control for potential microbial biotransformation. Blank samples from the 10 mM NaOH and HCl stock solutions were sampled at 0 and 18 d. The pH of each dark and light exposed sample was measured after the 18 d. The pH of the BEO samples dropped slightly from initial, ranging from 10.9 – 11.1, while after the 18 d the pH of the AEO samples was 2.3. A second round of photolysis and control experiments were carried out in an identical manner for the filtered OSPW (50 mg/L in 10 mM NaOH). OSPW pH measured 8.7 at the start of the experiment and 8.9 after 18 d. Absorption spectra (200-400 nm) of all three sample types were measured at Day 0 and Day 18 of irradiation (Figure S2).

2.4. Instrumental analysis

Triplicate sub-samples collected on each of Day 0, 5, 10, and 18 were analyzed by reverse phase liquid chromatography on an Accela HPLC system coupled to a hybrid linear ion-trap Orbitrap Elite mass spectrometer (Thermo Scientific, San Jose, CA) using elution conditions modified from Pereira et al.[43] Analyte separation was achieved on a Hypersil Gold C18 Selectivity Column (50 × 2.1 mm, 1.9 µm d.p., Thermo Scientific) under gradient conditions using a mobile phase composed of 0.1% acetic acid in water (A solvent) and 100 % methanol (B solvent) at a flow rate of 0.5 mL min^{-1}. The initial conditions of 95:5 (A:B) were held for 0.5 min. before being changed linearly to 10:90 (A:B) over 10 min, followed by a final ramp to 1:99 (A:B) over 5 min. Mobile phase composition was returned to initial conditions over 2.5 min and held for 2 min to allow the column to re-equilibrate. The column was maintained at 40 °C throughout the duration of the run. For all samples, 10 µL injection volumes were used.

All samples were analyzed in both positive (+) and negative (-) modes using APCI. The AEO samples were run in negative mode only to focus on organic acids, while BEO samples were run in positive mode only to focus on organic bases (e.g., N species) and non-ionic polar organics (e.g., alcohols, ketones). Mass spectral data was acquired in full scan between 100 and 500 *m/z* at a nominal resolution of 240,000 at *m/z* 400. Achieved resolutions ranged from >200,000 at *m/z* <150 to >120,000 at *m/z* ≤350.[17] Given that *m/z* ≤350 represents the majority of ions measured in this work, our method had sufficient resolving power to, for example, separate the commonly encountered mass split of 3.4 mDa.[44] Capillary temperature was 300°C, needle voltage was set to 2.25 kV, and nitrogen sheath, auxiliary, and capillary gas flows were set to 20, 15, and 3 (arbitrary units), respectively. Mass spectrometer calibration and additional operating conditions are described elsewhere.[17]

2.5. Data acquisition and handling

Xcalibur® software (Thermo Scientific, San Jose, CA) was used for instrument control, data acquisition, mass spectral interpretation, and assignment of molecular formulas. The total mass spectrum (*m/z*=100 to 500) was extracted over the retention time window in which the majority of species eluted (3-13 min). Empirical formulas were assigned from the exact mass of all detected species in both negative and positive modes (i.e. $C_vH_wO_xN_yS_z^{\pm}$) with the following restrictions: minimum (C-5, H-10), maximum (N-1, S-1, O-6), and a maximum mass accuracy error for formula prediction of 5 ppm.

Data from individual samples and blanks were organized and aligned across each triplicate set based on identical molecular formulas. Intensity measurements were then averaged across triplicates by molecular formula, blank-subtracted, and summed to determine total and heteroatomic class intensity values. For the negative mode samples, intensities were normalized to the internal standard signal. Positive mode samples were treated similarly except they were not normalized due to lack of an internal standard signal. Blank-subtracted values less than zero were considered equal to zero (i.e., for compounds/formulae where a greater signal was measured in the blank than the sample, the sample was considered to have a signal of zero for that particular compound/formula). Chemical species were then binned into the following 'classes' based on heteroatom content in in each of the two ionization modes: $O_2^{\pm}$, $O_3^{\pm}$, $O_4^{\pm}$, $O_5^{\pm}$, $O_6^{\pm}$, $SO^{\pm}$, $SO_2^{\pm}$, $SO_3^{\pm}$, $SO_4^{\pm}$, $SO_5^{\pm}$, $SO_6^{\pm}$, $NO^{\pm}$, $NO_2^{\pm}$ and $NO_3^{\pm}$. These are the predominant

classes identified in previous characterizations of OSPW[16,43,45,46] and include the most toxic classes.[5–8,47,48] All presented chemical formulae and DBE calculations are based on the empirical formula of the neutral compounds, rather than the protonated or deprotonated species detected.

First-order kinetics models were fit to data for whole OSPW (from both positive and negative mode measurements), as well as AEO and BEO samples (Tables S6 and S7). The peak intensity data was natural-log transformed and plotted as a ratio, $\ln[\text{intensity}_t / \text{intensity}_o]$ as a function of time (0, 5, 10, 18, d) to create first-order kinetic time-series plots. Two types of analyses were undertaken: In the first type (Type 1 analysis), first-order kinetic models were fit to the sum intensity of all molecular formulae within a heteroatomic class (e.g., all O_2^- species). In the second type (Type 2 analysis), to better compare degradation kinetics between sample types, first-order kinetic models were fit using only the intensity of individual species that were present in both whole OSPW and AEO, or whole OSPW and BEO. We further limited this comparison to only include species with an $R^2 > 0.1$. In both ionization modes the O_5S and O_6S classes had insufficient signal at all time points and could not be modelled by either type of kinetic analysis.

3. Results and Discussion

This study investigated the compositional changes that occurred within OSPW following 18 d of irradiation with λ>290 nm light. Overall, results for the isolated AEO and BEO samples were similar to those in whole OSPW, therefore, the following sections focus primarily on the compositional changes in whole OSPW, with AEO and BEO results discussed only when different from whole OSPW. Unless stated otherwise the data presented in the following discussions represents the mean ± standard deviation of triplicate samples.

3.1. Overall photodegradation of whole OSPW and OSPW-extracts

Exposure to light for 18 d resulted in reductions in the measured total ion intensity and total number of detected species in all samples (Figure S3 and Table S5). In negative mode, the sum total normalized intensities of dissolved organic species in whole OSPW and AEO samples were reduced by 97 ± 2% and 87 ± 3% respectively, over the course of the 18 d irradiation (Figure 1; Tables S1 and S2). A marked reduction in the total intensity in whole OSPW was observed after only 5 d, with intensities remaining relatively constant throughout the remainder

of the study period. In contrast to whole OSPW, the total intensity of AEO species remained relatively constant through the first 10 days of exposure. It was not until after Day 10 that a substantial reduction in intensity was observed in AEO, with the total intensities on Day 18 approaching those observed in whole OSPW (Figure 1). Organic species detected in positive mode were also extensively degraded by photolysis. The total ion intensity of whole OSPW was reduced by 73 ± 4% over the 18 d of exposure, comparatively less than observed in negative mode (Figures 1 and Table S3). Likewise, a reduction in total intensity in BEO from Day 0 to 18 was observed, albeit only by 53 ± 3% (Table S4). The total intensities of Dark and Dark kill control treatments at Day 0 and 18 were not significantly different from those in whole OSPW Day 0 samples in both positive and negative mode (Chi-square test, $p>0.05$), indicating that the reductions in irradiated treatments on Days 5, 10, and 18 samples resulted from photolysis.

The photodegradation of organic compounds in OSPW under environmentally-relevant conditions ($\lambda>290$ nm) has previously been reported to be negligible,[35,49] while other studies have reported reductions.[15,32] For example, Leshuk et al.[32] assessed the photocatalytic (TiO_2) degradation of AEOs in OSPW using natural sunlight by monitoring changes in chemical species profiles by HPLC-HRMS. A nearly complete removal of total AEO species was observed after 1 to 7 d equivalents of natural sunlight. Even in the absence of the TiO_2 catalyst, the authors noted reduction from 39.8 mg/L to 28.9 mg/L (27% depletion) over a one week-equivalent of natural sunlight and an approximately 10 to 15% depletion after only 1 day.[32] Likewise, Headley et al.[15] reported a nearly 75% reduction in the concentration of O_2^- species after 8 h of irradiation with natural sunlight in the presence of TiO_2, and a 10 to 15% reduction in the absence of a photocatalyst; as measured by low resolution mass spectrometry. In the same study, individual model compounds, such as 4-methylcyclohexane acetic acid ($C_9H_{16}O_2$) were also degraded by >50% under natural light conditions.[15] The extent of degradation reported herein exceeds those previously reported. The differences observed are likely due to the different experimental setups. While the aforementioned studies utilized natural sunlight,[15,32,35] here we utilized a bench-top reactor operating at an environmentally-relevant wavelength ($\lambda>290$ nm). The light intensity is greater in this study and wavelength distributions are considerably different from natural sunlight, the implications of which are described in Section 3.4, below. In addition, our exposure time of 18 d was longer than previous studies, which ranged from 8 hours to 7 d.[15,32,35]

Furthermore, we used APCI, in contrast to electrospray ionization (ESI) used in previous studies, which may result in ionization of a different range of species.[50]

Photodegradation was generally more extensive in whole OSPW than in either AEO or BEO samples (e.g., 97% reduction in intensity in whole OSPW versus 87% in AEO and 73% reduction in whole OSPW versus 52% in BEO). While elucidation of specific photolysis mechanisms was beyond the scope of this study, the presence of natural constituents (e.g., inorganic ions or other dissolved organic matter removed through preparation of AEO and BEO) in whole OSPW may have facilitated or enhanced indirect photolysis. Additionally, researchers have observed indirect aqueous photodegradation of OSPW O_2^- species and model O_2^- compounds facilitated by peroxyl or hydroxyl radicals.[51,52] Indirect photolysis is an important pathway for many organic contaminants that have limited absorption at wavelengths longer than 290 nm (i.e., reduced potential for direct photolysis).[25] For example, the presence of NO_3^-, Fe^{3+}, and humic acid increased the photodegradation rates of estradiol and estrone through indirect photolysis.[53] Humic acid and inorganic ions are present in OSPW, but would likely be removed during the column washing step in reverse phase SPE extraction (inorganic ions) or be more strongly retained on the column and not eluted (humic substances); therefore, they may not be present in final AEO or BEO extracts. Although inorganic species in OSPW, such as Fe^{3+} and HCO_3^-, have been shown to inhibit the photocatalytic degradation of OSPW constituents for remediation,[31] future work should focus on identifying which dissolved organic or inorganic substances can affect natural photodegradation rates of these complex mixtures.

3.2. Heteroatomic class kinetics

Prior to photolysis, the heteroatomic chemical class profile of dissolved organic species in whole OSPW and AEO was dominated by the O_x^- classes (53% and 23%, respectively; Figure 2), particularly O_2^- and O_3^- classes, followed by sulfur-containing classes (i.e., O_2S^-, O_3S^-, and O_4S^-). This heteroatomic profile is consistent with the profile reported by others,[16,45,46] despite differences in the ionization method utilized in this study (i.e., APCI versus electrospray ionization in other studies). In positive mode, O_2^+ and O_3^+ heteroatomic classes comprised substantial proportions of the total intensity (66% and 19%, respectively) in whole OSPW and BEO prior to photolysis (Figure 3), although the OS^+, O_2S^+, and ON^+ classes also contributed substantially to overall signal intensity.

3.2.1. Negative mode analysis

Most of the investigated heteroatomic classes were highly susceptible to photodegradation and were significantly reduced in intensity by Day 5. Highly photolabile species were present in the O_2^-, O_3^-, O_4^-, O_2S^-, O_4S^-, and O_5S^- classes, which were degraded by 93% to 100% after only 5 d (Table S1). The O_x^- classes were degraded by 71% to 99% (98 ± 5% overall), while O_xS^- classes were degraded by 26% to 100% (87 ± 17% overall) by Day 18. The day-by-day changes in AEO heteroatomic classes were more variable than in whole OSPW. Specifically, the intensity of each heteroatomic class, with the exception of O_3^-, O_2S^-, O_4S^-, and O_6S^-, increased from the start of the exposure through to Day 5 by 14% to 556% (Figure 2). However, by Day 18, all AEO heteroatomic classes had reduced 24% to 100% relative to Day 0. Overall, there was a greater percent reduction across SO_x^- classes (97 to 100% among classes, 99 ± 0.4% overall) than O_x^- classes (24 to 88% among classes, 86 ± 3% overall) in AEO, consistent with whole OSPW. Previous studies have noted preferential photodegradation of sulfur-containing classes in OSPW[32,46] and suggested that these species are more photolabile than O_x species.[33] Similarly, there was a shift to fewer S- and N-containing species, and correspondingly more O-containing species, in light-sour crude oil following exposure to a SoLux halogen bulb (simulating 42% of natural sunlight intensity) and a UV lamp (λ=254 nm) for 5.5 weeks, presumably as a result of photo-induced oxidation.[54]

Differences in photodegradation rates between heteroatomic classes led to changes in the overall composition of whole OSPW with time. From Day 5 to 18, the proportions of heteroatomic classes in the whole OSPW were variable, but generally samples were dominated by O_2^-, O_3^-, O_4^-, and O_3S^- classes (Figure 2, Table S1). On Day 0, the most prominent heteroatomic classes were (in decreasing order): O_2^- (53%), O_3^- (23%), O_4^- (13%), O_2S^-(7%), and O_3S^-(2%). By Day 5, these classes comprised 8%, 43%, 29%, <1%, and 13% of the measured intensity, respectively. Thus, after only 5 d, there was an observed shift towards a greater proportion of O_3^- and O_4^- in whole OSPW, as well as an increase in the relative prominence of O_3S^- (Figure 2). By Day 18, O_3^- was the most prominent class (40% of intensity), but $O_3S^-$and O_6S^-represented 24% and 16% of normalized intensity, respectively, representing a further shift towards greater proportion of more oxygen-containing species, relative to Day 0 (Figure 2). Furthermore, the ratios of O_3^- and O_4^- species relative to O_2^- increased from 0.44 and 0.24,

respectively, on Day 0 to 3.1 and 0.26, respectively, by Day 18. Changes to the chemical profile of bitumen-derived organic species following uncatalyzed photodegradation has not been reported previously, although the formation of more oxygenated species has been reported in diluted bitumen and/or water accommodated fractions of petroleum, which when exposed to sunlight, resulted in the formation of more highly oxidized petroleum species.[54–57]

Across all whole OSPW heteroatomic classes in negative mode, the average apparent photolysis half-life was 10.3 ± 17.0 d (Table 1). There were no differences in mean half-lives between O_x^- and SO_x^- as groups (10.5 ± 17.6 d vs 7.8 ± 8.3 d, respectively), although half-lives amongst heteroatomic classes within each group varied, ranging from 6.2 ± 7.0 d (O_4^-) to 14.9 ± 24.7 d (O_3^-). The slower apparent degradation rate of O_3^- is consistent with the observed shift to greater proportions of O_3^- species as a percentage of overall intensity throughout the duration of the experiment. Half-lives of other major classes, e.g., O_2^- and SO_3^-, were not significantly different from one another (11.0 ± 11.1 d vs. 11.5 ± 10.4 d, respectively), nor were there any differences from any other heteroatomic classes, likely as a result of the wide range of degradation half-lives of individual species within each class.

3.2.2. Positive mode analysis

In positive mode, the extent of removal by heteroatomic classes in whole OSPW ranged from 68% to 100%, with an overall average removal of 75 ± 11%. A greater removal of mixed sulfur-oxygen containing classes (i.e., O_xS) than corresponding oxygen (i.e., O_x) or nitrogen-containing classes (i.e., O_xN) was observed, with 99 ± 0.4% removal for O_xS versus 72 ± 15% and 80 ± 3% for O_x and O_xN classes, respectively. In general, a greater recalcitrance was observed for classes detected in positive mode compared to negative mode (e.g., O_2^+ reduced by 69 ± 22% versus O_2^- reduced by 99 ± 1% by Day 18), consistent with previous observations made for ozonated OSPW.[58] Likewise, for BEO species, the percent removal ranged from 31% to 99% across all heteroatomic groups, with the greatest percent removals observed for sulfur-containing classes (Table S4). The O_2^+, OS^+, and ON^+ classes (three of the presumed most toxic classes[8]) were ultimately degraded in BEO by 50 ± 4%, 98 ± 1%, and 75 ± 1% (respectively) by Day 18; however, there was evidence for the production (i.e., an increase in intensity response relative to Day 0 or Day 5) of O_2^+ and OS^+ species on Days 5 and 10 (Table S3 and S4) in BEO and whole OSPW samples.

Overall the apparent half-life for all classes detected in whole OSPW in positive mode was 10.8 ± 17.6 d, similar to the overall half-life observed in negative mode. In contrast to negative mode whole OSPW classes, the half-lives of sulfur-containing classes were significantly shorter than for the corresponding O_x^+ or NO_x^+ classes (Table 1 and Tables S6 and S7), corroborating our previous finding that O_xS^+ compounds overall were more extensively degraded than either O_x^+ or NO_x^+ compounds. Similarly, half-lives of individual heteroatomic classes followed a similar trend. For example, half-lives of O_3S^+ (3.9 ± 1.5 d) were significantly shorter than for either O_3^+ (8.3 ± 10.0 d) or O_3N^+ (13.2 ± 13.6 d)—a trend consistently observed among other individual heteroatomic classes as well.

3.2.3. All species

We further found differences in degradation kinetics of heteroatomic classes between dissolved organics species in whole OSPW compared to either AEO or BEO, consistent with the overall trends discussed above (Figure 1). When considering all species present in either whole OSPW or AEO (i.e, Type 1 analysis), there were no differences in mean half-lives between the two sample types. However, when considering only species detected in both whole OSPW and AEO or BEO samples (i.e., Type 2 analysis), degradation was consistently faster across heteroatomic classes in whole OSPW than in either AEO or BEO. For example, the mean half-lives for individual species of the O_2^- class present in both whole OSPW and AEO were 11.7 ± 5.6 d (AEO) compared to only 1.9 ± 0.6 d for the same species in whole OSPW. Similar trends exist for other negative mode species as well (Tables S6 and S7), and the trend was further exacerbated when narrower criteria (i.e., R^2>0.5) was applied. Overall, for species detected in negative mode and present in both whole OSPW and AEO, degradation in whole OSPW was, on average, 2 times faster than in AEO samples. In positive mode, degradation was 2.5 times slower for BEO species than whole OSPW species (Table S7), consistent with our finding for whole OSPW and AEO species above. As mentioned previously, the differences observed between whole OSPW and either AEO or BEO may be due to indirect photolysis facilitated by species that were removed through the SPE extraction procedure.

In Table 1 and Table S6 and S7 we note significant differences in degradation kinetics for some of the same heteroatom classes detected in whole OSPW by the two ionization modes. For example, OSPW O_3^+ vs O_3^- have half-lives of 8 and 15 d, respectively (Table 1) and paired

OSPW O_2^+ vs O_2^- species have half-lives of 13 and 2 d, respectively (Table S6 and S7). This is not surprising because the structures/functional groups of these species are believed to be different in the different ionization modes. For example, the O_2^- class contains a complex mixture of carboxylic acids (i.e., naphthenic acids) whose core structures are largely undefined but may include alkyl, cycloaliphatic, double-bonds, or aromatic moieties. The O_2^+ group, on the other hand, have different retention times by HPLC (even for the same molecular formula) and are non-ionic polar organics whose oxygen atoms are incorporated into the structure as ketones or alcohols.[17,58]

3.2.4. Kinetics of Individual Species

The photodegradation behavior of individual OSPW species detected in negative ionization mode varied. The majority of species degraded throughout the experiment (Figures 4A and B), consistent with expected first-order photodegradation. However, other species were produced linearly over irradiation time (Figure 4C), suggesting that these species were formed as products from phototransformation of other species. Moreover, some species were initially degraded, but later produced (Figures 4D and 4E), or vice versa whereby a compound was initially formed but subsequently degraded (Figure 4F). Such selected kinetics plots, as well as the compositional changes of individual chemical species over time shown in the heat maps (Figure S4), demonstrate the variation of photochemical changes taking place within the complex mixture of whole OSPW species, and that chemical kinetics are both class- and species-specific.

3.3. Carbon number and DBE trends

Irradiation treatment produced observable changes to the carbon number and DBE profiles within individual heteroatomic classes for all samples analyzed. For all species detected in negative mode, whole OSPW samples had a mean carbon number of 15 and mean DBE of 5 on Day 0. Following 18 d of exposure, mean carbon number and DBE decreased to 12 and 3, respectively, indicating preferential degradation of larger species with more rings or double bonds. Furthermore, when reductions on Day 18 were compared across all carbon numbers and DBE values in whole OSPW, an increased response of some species with DBE=2, and with between 7-9 carbons was observed, suggesting formation from the photodegradation of other species. The distribution of carbon and DBE values in AEO at Day 0 were similar to those

observed in whole OSPW in negative mode, whereby species contained 10-20 carbons and had DBE values of 2-13. However, in AEO samples, there was a lack of the 7 to 9-carbon species observed in whole OSPW, likely as a result of not being retained during the SPE extraction. By Day 18, AEO contained a similar distribution of carbons and DBE as observed on Day 0, and also contained species with 7-9 carbons, indicating that these smaller compounds could indeed be formed during the photolysis.

Similar trends were observed within specific heteroatomic classes. Prior to photolysis, blank-subtracted whole OSPW contained O_2^- species with 7 to 20 carbons and 2 to 12 DBE (Figure S3), with the most abundant species being O_2^- species with DBE = 4: $C_{14}H_{22}O_2$ and $C_{15}H_{24}O_2$, consistent with previously reported OSPW profiles.[16] Throughout the 18-day irradiation, a decrease in the intensity of species between 12 and 18 carbons and DBE>3 was observed (Figure 5). This observation was corroborated by a general trend towards faster degradation (i.e., shortest half-lives) of O_x^- species in whole OSPW with 4 to 8 DBEs (Table S8), which was the heteroatomic class that most commonly met the data requirements for applying first-order kinetic models (minimum of three time points). Species with DBE>5 may contain aromatic functional groups which could enhance photon absorption and increase the rate of photodegradation. Moreover, this finding is consistent with previous findings where exposure of OSPW-derived AEO to natural and artificial sunlight induced a change in mixture composition towards an increase in smaller molecular weight compounds, although these measurements by low-resolution mass spectrometry do not allow differentiation of the various chemical classes.[35] Similarly, individual OSPW AEO species with greater DBE and carbon numbers were preferentially degraded by ozonation, resulting in a reduction in mean carbon and DBE values.[58] The degradation of larger species with more DBE, and the subsequent increase in intensity of smaller species with fewer DBE was observed for other heteroatomic classes in both positive and negative mode in the current work (Figures S3 and S4).

In positive mode, whole OSPW and BEO contained species with carbon numbers ranging from 6 to 29 and DBE from 2 to 15 on Day 0. On Day 18, little change in the distribution of carbon number and DBE was observed, with carbon numbers ranging from 6 to 28 and DBE from 2 to 14 (Figures S3 and S4). This result is consistent with the comparatively lower removal percentage for species in positive mode compared to those observed in negative mode. The

degradation of individual species, relative to D0, can nevertheless be observed within each heteroatomic class in the heat maps (Figure S4).

3.4. Natural sunlight extrapolations

Although the photoreactor employed in these studies represents an environmentally relevant light source (i.e., wavelengths <290 nm are filtered out) and therefore provides insight to compositional changes of OSPW mixtures subject to photolysis in the real-world, the wavelength distribution and light intensity is different from natural sunlight. Additionally, test tube photolysis experiments do not accurately account for light screening effects occurring in typical surface waters. Therefore, the reported laboratory half-lives here (Table S6 and S7) cannot be directly equated with environmental half-lives. However, using tabulated solar irradiance data at various seasons and our previous work comparing laboratory and natural sunlight (50 °N latitude) photolysis,[37] we can extrapolate the laboratory derived half-lives to natural sunlight conditions that are representative of those in the Athabasca oil sands region (57 °N).

Based on extrapolated laboratory data from Lu et al.[37] (using the same photoreactor) at 50 °N latitude in spring, summer, and fall, the light intensity from our laboratory photoreactor is approximately 13 (summer) to 40 (fall) times higher than natural sunlight. Based on this, natural sunlight half-lives for OSPW organic species at 57 °N latitude are estimated to be in the range of 122 d in summer to 384 d in fall (average of all OSPW chemical classes, Table 1). These estimates are consistent with overall degradation half-lives of 221 to 286 d for OSPW-derived AEOs reported from summer studies using natural sunlight and conducted in Saskatoon, Saskatchewan (52 °N).[35] However, the McMartin et al. data[35] was acquired using a low resolution mass spectrometer in negative ESI mode, so more detailed comparisons to our high mass resolution data are difficult.

These natural sunlight half-life estimates should be treated with caution as there is inherent uncertainty involved in using a model compound to extrapolate our photoreactor light intensity to natural sunlight intensity. With these specific extrapolations, it is critical that our whole OSPW extracts have a similar spectral overlap with the model compound used by Lu et al.[37] (thiamethoxam). Indeed, both whole OSPW and thiamethoxam both exhibit tailing

absorbance over wavelengths longer than 290 nm (Figure S2), with no major absorbance peaks overlapping the UV-B and UV-A ranges, making it a sufficient model compound.

It is also important to note that the spring, summer, and fall half-lives reported in Table 1 only apply to near surface photolysis, and do not account for light screening at depth, which is an extremely important factor and dependent upon the surface water.[37,59,60] Previous work estimated a light screening factor of the mesocosm water referenced below to be 0.45 to 0.69 in the 290 to 360 nm wavelength range,[41] which is typical for many natural surface waters.[60] However, the mesocosm extrapolations presented here (Table 1) utilize actual light intensity measurements taken at different depths (surface, 8, 18, and 28 cm)[37] The surface measured half-life (<1 cm below surface) for thiamethoxam measured outdoors in July (Winnipeg, MB, Canada, 49.9 °N) was 64 times slower than the laboratory measured half-life and 5 times slower compared to the summer estimation using tabulated solar irradiance data. Again, using thiamethoxam as a model compound for extrapolations, applying this ≈5-fold difference between summer and mesocosm half-lives to our whole OSPW extracts, we get the mesocosm half-life values presented in Table 1. This difference between summer and mesocosm degradation, in part, is a result of the light screening occurring at the surface of the mesocosm water. This screening becomes even more drastic at depths, with reductions in sunlight flux nearing 89% and 98% at 8 and 18 cm depths.[37] Thus, the mesocosm half-live estimates (Table 1) are likely the most applicable to the water bodies where bitumen-derived dissolved organic species typically occur.

3.5. Environmental significance

This study demonstrated that dissolved organic species in OSPW may be photodegraded, contrasting previous suggestions that photolysis was not a significant natural transformation pathway for these compounds. While specific attenuation rates would depend on the hydrology and environmental conditions of individual water bodies, these findings may be most relevant to informing the design of end-pit lakes, one of the reclamation strategies put forward by the Alberta government to promote healthy aquatic ecosystems and store OSPW and fluid fine tailings (FFT).[61] As end-pit lakes are proposed as the primary long-term solution for the remediation of oil sands tailings ponds, our results suggest that long-term exposure to solar radiation may provide a possible avenue for degradation and detoxification of OSPW dissolved organic species. However, end-pit lakes can have extremely high turbidity,[61] and light screening

480 is a critical consideration. Base-Mine Lake is one such example of an end-pit design that suffers
481 from extremely high turbidity and poor light penetration, a result of resuspension of the 45m
482 deep FFT bottom layer into the 8.5 m top OSPW layer.[61] Based on our data, these scenarios
483 would greatly reduce the extent of photolysis occurring in these lakes and limit the potential for
484 natural photo-remediation of OSPW. Our results suggest that natural photolysis may be an
485 important mechanism for allowing efficient OSPW remediation, but the effectiveness of this
486 process will depend on careful design of lake morphology and reducing turbidity to allow greater
487 light penetration. We therefore suggest that future end-pit lakes be shallow to maximize the
488 potential for natural photolysis to assist in remediation of OSPW. It is also plausible that OSPW
489 that is photodegraded at the near-surface will be mixed further down into the water column, and
490 fresh OSPW migrate to the near-surface to be photodegraded, allowing for continued photo-
491 induced attenuation of OSPW in end-pit lakes.

492

493 **Acknowledgements**

494 Thank you to the three anonymous reviewers for taking their time to review our manuscript and
495 provide helpful comments that contributed to the improvement of this manuscript. We
496 acknowledge the support of the Natural Sciences and Engineering Research Council of Canada
497 (NSERC), through funding of Discovery grants to MSR [funding reference number RGPIN-2015-
498 04852] and CSW [funding reference number RGPIN-2018-05542], a Vanier Scholarship to JKC,
499 and the Canada Research Chairs Program to CSW.

500

References

1 R. J. Mikula, V. A. Munoz and O. Omotoso, Water Use in Bitumen Production: Tailings Management in Surface Mined Oil Sands, , DOI:10.2118/2008-097.

2 P. Gosselin, S. E. Hrudey, M. A. Naeth, A. Plourde, R. Therrien, G. Van Der Kraak and Z. Xu, *Environmental and Health Impacts of Canada's Oil Sands Industry*, 2010.

3 P. R. Kannel and T. Y. Gan, Naphthenic acids degradation and toxicity mitigation in tailings wastewater systems and aquatic environments: A review, *J. Environ. Sci. Heal. Part A*, 2012, **47**, 1–21.

4 J. S. Clemente and P. M. Fedorak, A review of the occurrence, analyses, toxicity, and biodegradation of naphthenic acids, *Chemosphere*, 2005, **60**, 585–600.

5 F. M. Holowenko, M. D. MacKinnon and P. M. Fedorak, Characterization of naphthenic acids in oil sands wastewaters by gas chromatography-mass spectrometry, *Water Res.*, 2002, **36**, 2843–2855.

6 L. D. Brown and A. C. Ulrich, Oil sands naphthenic acids: A review of properties, measurement, and treatment, *Chemosphere*, 2015, **127**, 276–290.

7 J. Anderson, S. B. Wiseman, A. Moustafa, M. Gamal El-Din, K. Liber and J. P. Giesy, Effects of exposure to oil sands process-affected water from experimental reclamation ponds on Chironomus dilutus, *Water Res.*, 2012, **46**, 1662–1672.

8 G. D. Morandi, S. B. Wiseman, A. Pereira, R. Mankidy, I. G. M. Gault, J. W. Martin and J. P. Giesy, Effects-Directed Analysis of Dissolved Organic Compounds in Oil Sands Process-Affected Water, *Environ. Sci. Technol.*, 2015, **49**, 12395–12404.

9 M. P. Barrow, K. M. Peru, B. Fahlman, L. M. Hewitt, R. A. Frank and J. V Headley, Beyond Naphthenic Acids: Environmental Screening of Water from Natural Sources and the Athabasca Oil Sands Industry Using Atmospheric Pressure Photoionization Fourier Transform Ion Cyclotron Resonance Mass Spectrometry, *J. Am. Soc. Mass Spectrom.*, 2015, **26**, 1508–1521.

10 S. J. Rowland, C. E. West, D. Jones, A. G. Scarlett, R. A. Frank and L. M. Hewitt, Steroidal Aromatic 'Naphthenic Acids' in Oil Sands Process-Affected Water: Structural Comparisons with Environmental Estrogens, *Environ. Sci. Technol.*, 2011, **45**, 9806–9815.

11 S. J. Rowland, A. G. Scarlett, D. Jones, C. E. West and R. a Frank, Diamonds in the rough: identification of individual naphthenic acids in oil sands process water., *Environ. Sci. Technol.*, 2011, **45**, 3154–3159.

12 J. V. Headley, K. M. Peru, M. H. Mohamed, R. A. Frank, J. W. Martin, R. R. O. Hazewinkel, D. Humphries, N. P. Gurprasad, L. M. Hewitt, D. C. G. Muir, D. Lindeman, R. Strub, R. F. Young, D. M. Grewer, R. M. Whittal, P. M. Fedorak, D. A. Birkholz, R. Hindle, R. Reisdorph, X. Wang, K. L. Kasperski, C. Hamilton, M. Woudneh, G. Wang, B. Loescher, A. Farwell, D. G. Dixon, M. Ross, A. Dos Santos Pereira, E. King, M. P. Barrow, B. Fahlman, J. Bailey, D. W. McMartin, C. H. Borchers, C. H. Ryan, N. S. Toor, H. M. Gillis, L. Zuin, G. Bickerton, M. McMaster, E. Sverko, D. Shang, L. D. Wilson and

F. J. Wrona, Chemical fingerprinting of naphthenic acids and oil sands process waters-A review of analytical methods for environmental samples, *J. Environ. Sci. Heal. - Part A Toxic/Hazardous Subst. Environ. Eng.*, 2013, **48**, 1145–1163.

13 D. M. Grewer, R. F. Young, R. M. Whittal and P. M. Fedorak, Naphthenic acids and other acid-extractables in water samples from Alberta: What is being measured?, *Sci. Total Environ.*, 2010, **408**, 5997–6010.

14 J. V Headley, K. M. Peru, S. A. Armstrong, X. Han, J. W. Martin, M. M. Mapolelo, D. F. Smith, R. P. Rogers and A. G. Marshall, Aquatic plant-derived changes in oil sands naphthenic acid signatures determined by low-, high- and ultrahigh-resolution mass spectrometry, *Rapid Commun. Mass Spectrom.*, 2009, **23**, 515–522.

15 J. V Headley, J.-L. Du, K. M. Peru and D. W. McMartin, Electrospray ionization mass spectrometry of the photodegradation of naphthenic acids mixtures irradiated with titanium dioxide, *J. Environ. Sci. Heal. Part A*, 2009, **44**, 591–597.

16 M. P. Barrow, M. Witt, J. V Headley and K. M. Peru, Athabasca Oil Sands Process Water: Characterization by Atmospheric Pressure Photoionization and Electrospray Ionization Fourier Transform Ion Cyclotron Resonance Mass Spectrometry, *Anal. Chem.*, 2010, **82**, 3727–3735.

17 A. S. Pereira, S. Bhattacharjee and J. W. Martin, Characterization of Oil Sands Process-Affected Waters by Liquid Chromatography Orbitrap Mass Spectrometry, *Environ. Sci. Technol.*, 2013, **47**, 5504–5513.

18 J. V Headley, K. M. Peru, S. Mishra, V. Meda, A. K. Dalai, D. W. McMartin, M. M. Mapolelo, R. P. Rodgers and A. G. Marshall, Characterization of oil sands naphthenic acids treated with ultraviolet and microwave radiation by negative ion electrospray Fourier transform ion cyclotron resonance mass spectrometry, *Rapid Commun. Mass Spectrom.*, 2010, **24**, 3121–3126.

19 M. S. Ross, A. D. S. Pereira, J. Fennell, M. Davies, J. Johnson, L. Sliva and J. W. Martin, Quantitative and qualitative analysis of naphthenic acids in natural waters surrounding the canadian oil sands industry, *Environ. Sci. Technol.*, , DOI:10.1021/es303432u.

20 S. K. Lengger, A. G. Scarlett, C. E. West, R. A. Frank, L. M. Hewitt, C. B. Milestone and S. J. Rowland, Use of the distributions of adamantane acids to profile short-term temporal and pond-scale spatial variations in the composition of oil sands process-affected waters, *Environ. Sci. Process. Impacts*, 2015, **17**, 1415–1423.

21 R. A. Frank, C. B. Milestone, S. J. Rowland, J. V Headley, R. J. Kavanagh, S. K. Lengger, A. G. Scarlett, C. E. West, K. M. Peru and L. M. Hewitt, Assessing spatial and temporal variability of acid-extractable organics in oil sands process-affected waters, *Chemosphere*, 2016, **160**, 303–313.

22 J. M. E. Ahad, H. Pakdel, M. M. Savard, A. I. Calderhead, P. R. Gammon, A. Rivera, K. M. Peru and J. V Headley, Characterization and Quantification of Mining-Related "Naphthenic Acids" in Groundwater near a Major Oil Sands Tailings Pond, *Environ. Sci. Technol.*, 2013, **47**, 5023–5030.

23 S. J. Rowland, C. E. West, A. G. Scarlett, C. Ho and D. Jones, Differentiation of two industrial oil sands process-affected waters by two-dimensional gas chromatography/mass spectrometry of diamondoid acid profiles, *Rapid Commun. Mass Spectrom.*, 2012, **26**, 572–576.

24 J. V Headley, M. P. Barrow, K. M. Peru, B. Fahlman, R. A. Frank, G. Bickerton, M. E. McMaster, J. Parrott and L. M. Hewitt, Preliminary fingerprinting of Athabasca oil sands polar organics in environmental samples using electrospray ionization Fourier transform ion cyclotron resonance mass spectrometry, *Rapid Commun. Mass Spectrom.*, 2011, **25**, 1899–1909.

25 J. K. Challis, M. L. Hanson, K. J. Friesen and C. S. Wong, A critical assessment of the photodegradation of pharmaceuticals in aquatic environments: defining our current understanding and identifying knowledge gaps, *Environ. Sci. Process. Impacts*, 2014, **16**, 672–696.

26 C. Sun, W. Shotyk, C. W. Cuss, M. W. Donner, J. Fennell, M. Javed, T. Noernberg, M. Poesch, R. Pelletier, N. Sinnatamby, T. Siddique and J. W. Martin, Characterization of Naphthenic Acids and Other Dissolved Organics in Natural Water from the Athabasca Oil Sands Region, Canada, *Environ. Sci. Technol.*, 2017, **51**, 9524–9532.

27 R. A. Frank, J. W. Roy, G. Bickerton, S. J. Rowland, J. V Headley, A. G. Scarlett, C. E. West, K. M. Peru, J. L. Parrott, F. M. Conly and L. M. Hewitt, Profiling Oil Sands Mixtures from Industrial Developments and Natural Groundwaters for Source Identification, *Environ. Sci. Technol.*, 2014, **48**, 2660–2670.

28 S. A. Stout and Z. Wang, in *Standard Handbook Oil Spill Environmental Forensics: Fingerprinting and Source Identification*, eds. S. A. Stout and Z. B. T.-S. H. O. S. E. F. (Second E. Wang, Academic Press, Boston, 2nd edn., 2016, pp. 61–129.

29 C. B. T.-A. in A. M. Whitby, in *Advances in Applied Microbiology*, Academic Press, 2010, vol. 70, pp. 93–125.

30 R. C. Prince, R. M. Garrett, R. E. Bare, M. J. Grossman, T. Townsend, J. M. Suflita, K. Lee, E. H. Owens, G. A. Sergy, J. F. Braddock, J. E. Lindstrom and R. R. Lessard, The Roles of Photooxidation and Biodegradation in Long-term Weathering of Crude and Heavy Fuel Oils, *Spill Sci. Technol. Bull.*, 2003, **8**, 145–156.

31 T. Leshuk, D. de Oliveira Livera, K. M. Peru, J. V Headley, S. Vijayaraghavan, T. Wong and F. Gu, Photocatalytic degradation kinetics of naphthenic acids in oil sands process-affected water: Multifactorial determination of significant factors, *Chemosphere*, 2016, **165**, 10–17.

32 T. Leshuk, T. Wong, S. Linley, K. M. Peru, J. V Headley and F. Gu, Solar photocatalytic degradation of naphthenic acids in oil sands process-affected water, *Chemosphere*, 2016, **144**, 1854–1861.

33 D. de Oliveira Livera, T. Leshuk, K. M. Peru, J. V Headley and F. Gu, Structure-reactivity relationship of naphthenic acids in the photocatalytic degradation process, *Chemosphere*, 2018, **200**, 180–190.

34 S. Mishra, V. Meda, A. K. Dalai, D. W. McMartin, J. V. Headley and K. M. Peru, Photocatalysis of Naphthenic Acids in Water, *J. Water Resour. Prot.*, 2010, **02**, 644–650.

35 D. W. McMartin, J. V Headley, D. A. Friesen, K. M. Peru and J. A. Gillies, Photolysis of Naphthenic Acids in Natural Surface Water, *J. Environ. Sci. Heal. Part A*, 2004, **39**, 1361–1383.

36 M. D. MacKinnon and H. Boerger, Description of Two Treatment Methods for Detoxifying Oil Sands Tailings Pond Water, *Water Qual. Res. J.*, 1986, **21**, 496–512.

37 Z. Lu, J. K. Challis and C. S. Wong, Quantum Yields for Direct Photolysis of Neonicotinoid Insecticides in Water: Implications for Exposure to Nontarget Aquatic Organisms, *Environ. Sci. Technol. Lett.*, 2015, **2**, 188–192.

38 D. Jones, C. E. West, A. G. Scarlett, R. A. Frank and S. J. Rowland, Isolation and estimation of the 'aromatic' naphthenic acid content of an oil sands process-affected water extract, *J. Chromatogr. A*, 2012, **1247**, 171–175.

39 D. Jones, A. G. Scarlett, C. E. West, R. A. Frank, R. Gieleciak, D. Hager, J. Pureveen, E. Tegelaar and S. J. Rowland, Elemental and spectroscopic characterization of fractions of an acidic extract of oil sands process water, *Chemosphere*, 2013, **93**, 1655–1664.

40 M. P. Barrow, K. M. Peru, D. W. McMartin and J. V Headley, Effects of Extraction pH on the Fourier Transform Ion Cyclotron Resonance Mass Spectrometry Profiles of Athabasca Oil Sands Process Water, *Energy & Fuels*, 2016, **30**, 3615–3621.

41 J. K. Challis, J. C. Carlson, K. J. Friesen, M. L. Hanson and C. S. Wong, Aquatic photochemistry of the sulfonamide antibiotic sulfapyridine, *J. Photochem. Photobiol. A Chem.*, 2013, **262**, 14–21.

42 J. N. Apell and K. McNeill, Updated and validated solar irradiance reference spectra for estimating environmental photodegradation rates, *Environ. Sci. Process. Impacts*, 2019, **21**, 427–437.

43 A. S. Pereira and J. W. Martin, On-Line Solid Phase Extraction – HPLC – Orbitrap Mass Spectrometry for Screening and Quantifying Targeted and Non-Targeted Analytes in Oil Sands Process-Affected Water and Natural Waters in the Athabasca Oil Sands Region, *Oil Sands Res. Inf. Netw. Tech. Reports*, 2014, OSRIN Report No. TR-45.

44 A. G. Marshall, Milestones in fourier transform ion cyclotron resonance mass spectrometry technique development, *Int. J. Mass Spectrom.*, 2000, **200**, 331–356.

45 T. Leshuk, K. M. Peru, D. de Oliveira Livera, A. Tripp, P. Bardo, J. V Headley and F. Gu, Petroleomic analysis of the treatment of naphthenic organics in oil sands process-affected water with buoyant photocatalysts, *Water Res.*, 2018, **141**, 297–306.

46 C. Wang, R. Huang, N. Klamerth, P. Chelme-Ayala and M. Gamal El-Din, Positive and negative electrospray ionization analyses of the organic fractions in raw and oxidized oil sands process-affected water, *Chemosphere*, 2016, **165**, 239–247.

47 S. A. Hughes, A. Mahaffey, B. Shore, J. Baker, B. Kilgour, C. Brown, K. M. Peru, J. V Headley and H. C. Bailey, Using ultrahigh-resolution mass spectrometry and toxicity

identification techniques to characterize the toxicity of oil sands process-affected water: The case for classical naphthenic acids, *Environ. Toxicol. Chem.*, 2017, **36**, 3148–3157.

48 G. D. Morandi, S. B. Wiseman, M. Guan, X. W. Zhang, J. W. Martin and J. P. Giesy, Elucidating mechanisms of toxic action of dissolved organic chemicals in oil sands process-affected water (OSPW), *Chemosphere*, 2017, **186**, 893–900.

49 Z. Shu, C. Li, M. Belosevic, J. R. Bolton and M. G. El-Din, Application of a Solar UV/Chlorine Advanced Oxidation Process to Oil Sands Process-Affected Water Remediation, *Environ. Sci. Technol.*, 2014, **48**, 9692–9701.

50 S. J. Rowland, A. S. Pereira, J. W. Martin, A. G. Scarlett, C. E. West, S. K. Lengger, M. J. Wilde, J. Pureveen, E. W. Tegelaar, R. A. Frank and L. M. Hewitt, Mass spectral characterisation of a polar, esterified fraction of an organic extract of an oil sands process water, *Rapid Commun. Mass Spectrom.*, 2014, **28**, 2352–2362.

51 P. Drzewicz, A. Afzal, M. G. El-Din and J. W. Martin, Degradation of a Model Naphthenic Acid, Cyclohexanoic Acid, by Vacuum UV (172 nm) and UV (254 nm)/H2O2, *J. Phys. Chem. A*, 2010, **114**, 12067–12074.

52 A. Afzal, P. Drzewicz, L. A. Pérez-Estrada, Y. Chen, J. W. Martin and M. Gamal El-Din, Effect of Molecular Structure on the Relative Reactivity of Naphthenic Acids in the UV/H2O2 Advanced Oxidation Process, *Environ. Sci. Technol.*, 2012, **46**, 10727–10734.

53 R. R. Chowdhury, P. Charpentier and M. B. Ray, Photodegradation of Estrone in Solar Irradiation, *Ind. Eng. Chem. Res.*, 2010, **49**, 6923–6930.

54 M. T. Griffiths, R. Da Campo, P. B. O'Connor and M. P. Barrow, Throwing Light on Petroleum: Simulated Exposure of Crude Oil to Sunlight and Characterization Using Atmospheric Pressure Photoionization Fourier Transform Ion Cyclotron Resonance Mass Spectrometry, *Anal. Chem.*, 2014, **86**, 527–534.

55 Z. Yang, G. Zhang, B. P. Hollebone, C. E. Brown, C. Yang, P. Lambert, Z. Wang, M. Landriault and K. Shah, Fate of oxygenated intermediates in solar irradiated diluted bitumen mixed with saltwater, *Environ. Pollut.*, 2017, **231**, 622–634.

56 P. Benigni, K. Sandoval, C. J. Thompson, M. E. Ridgeway, M. A. Park, P. Gardinali and F. Fernandez-Lima, Analysis of Photoirradiated Water Accommodated Fractions of Crude Oils Using Tandem TIMS and FT-ICR MS, *Environ. Sci. Technol.*, 2017, **51**, 5978–5988.

57 P. Z. Ray, H. Chen, D. C. Podgorski, A. M. McKenna and M. A. Tarr, Sunlight creates oxygenated species in water-soluble fractions of Deepwater horizon oil, *J. Hazard. Mater.*, 2014, **280**, 636–643.

58 A. S. Pereira, M. S. Islam, M. G. El-Din and J. W. Martin, Ozonation degrades all detectable organic compound classes in oil sands process-affected water; an application of high-performance liquid chromatography/obitrap mass spectrometry., *Rapid Commun. Mass Spectrom.*, 2013, **27**, 2317–2326.

59 J. J. Guerard, P. L. Miller, T. D. Trouts and Y.-P. Chin, The role of fulvic acid composition in the photosensitized degradation of aquatic contaminants, *Aquat. Sci.*, 2009, **71**, 160–169.

60 M. W. Lam and S. A. Mabury, Photodegradation of the pharmaceuticals atorvastatin, carbamazepine, levofloxacin, and sulfamethoxazole in natural waters, *Aquat. Sci.*, 2005, **67**, 177–188.

61 P. H. Yin, B. J. T., Y. Xiaoxuan and U. A. C., Turbidity Mitigation in an Oil Sands Pit Lake through pH Reduction and Fresh Water Addition, *J. Environ. Eng.*, 2018, **144**, 4018127.

Figures

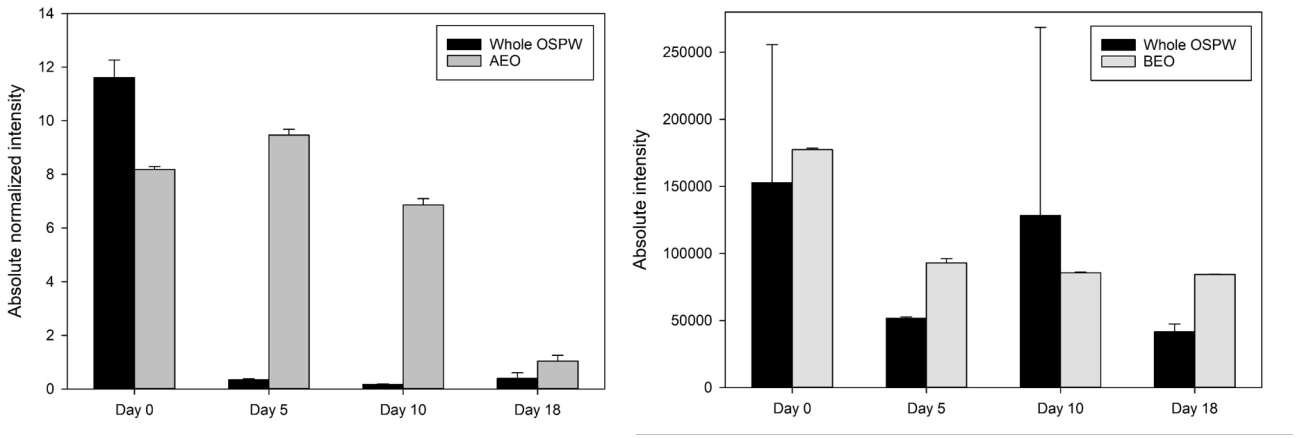

Figure 1: Mean (±SD) total ion intensity in negative mode [A] and positive mode [B] in whole OSPW and acid-extractable organic (AEO), and base-extractable organic (BEO) samples (n=2-3) on days 0, 5, 10, and 18 of irradiation. All data are blank subtracted. Note that the intensity scales are different between figures, as negative mode data [A] have been normalized to the intensity of the internal standard.

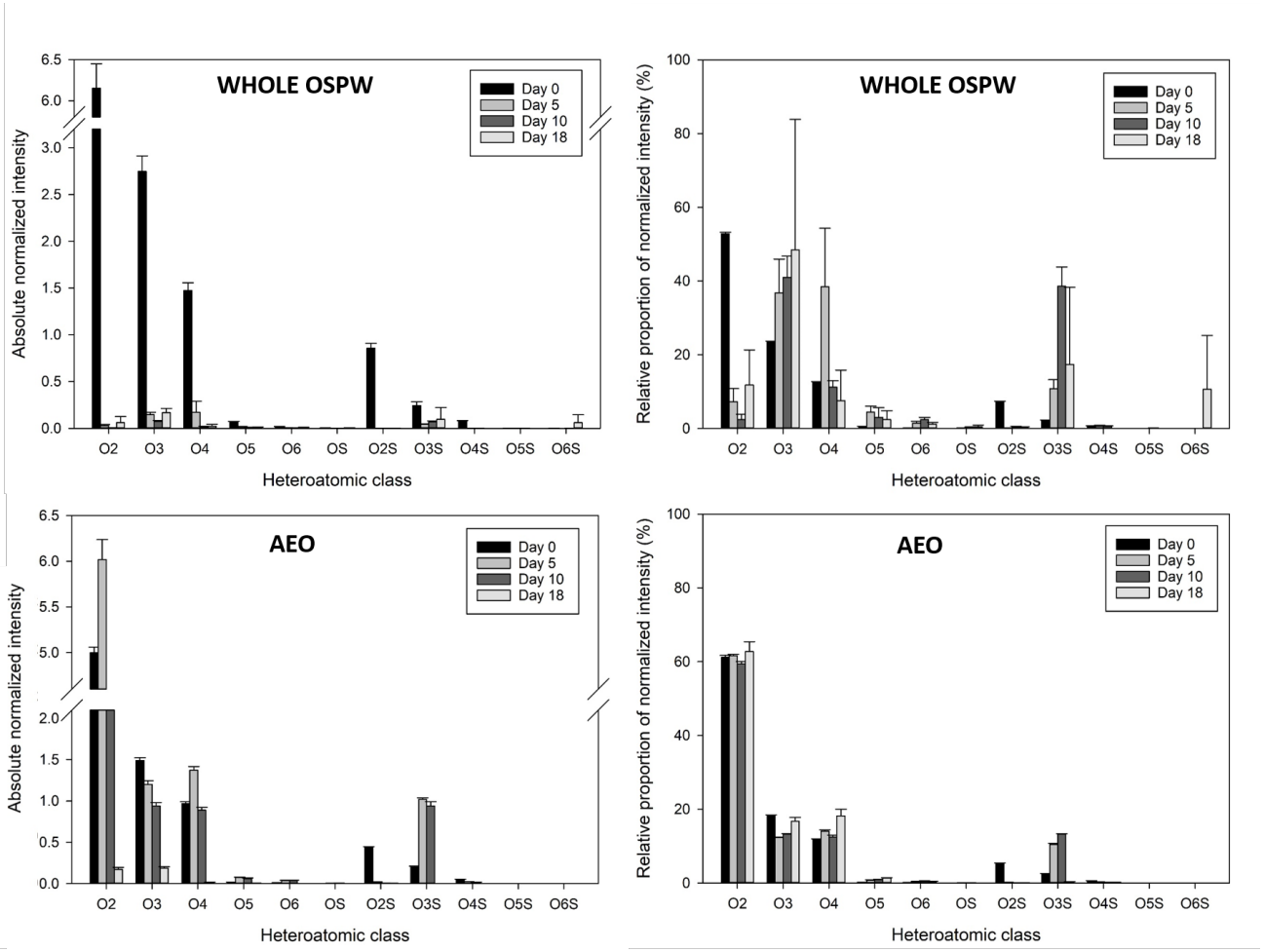

Figure 2: Mean (±SD) negative mode intensity by heteroatomic class as absolute (left) and relative (proportion of total sample response) intensities (right) on Days 0, 5, 10 and 18 of irradiation in OSPW (top) and acid-extractable organics (AEO) samples (bottom) (n=2-3). All sample intensities are blank-subtracted and normalized to the intensity of the internal standard.

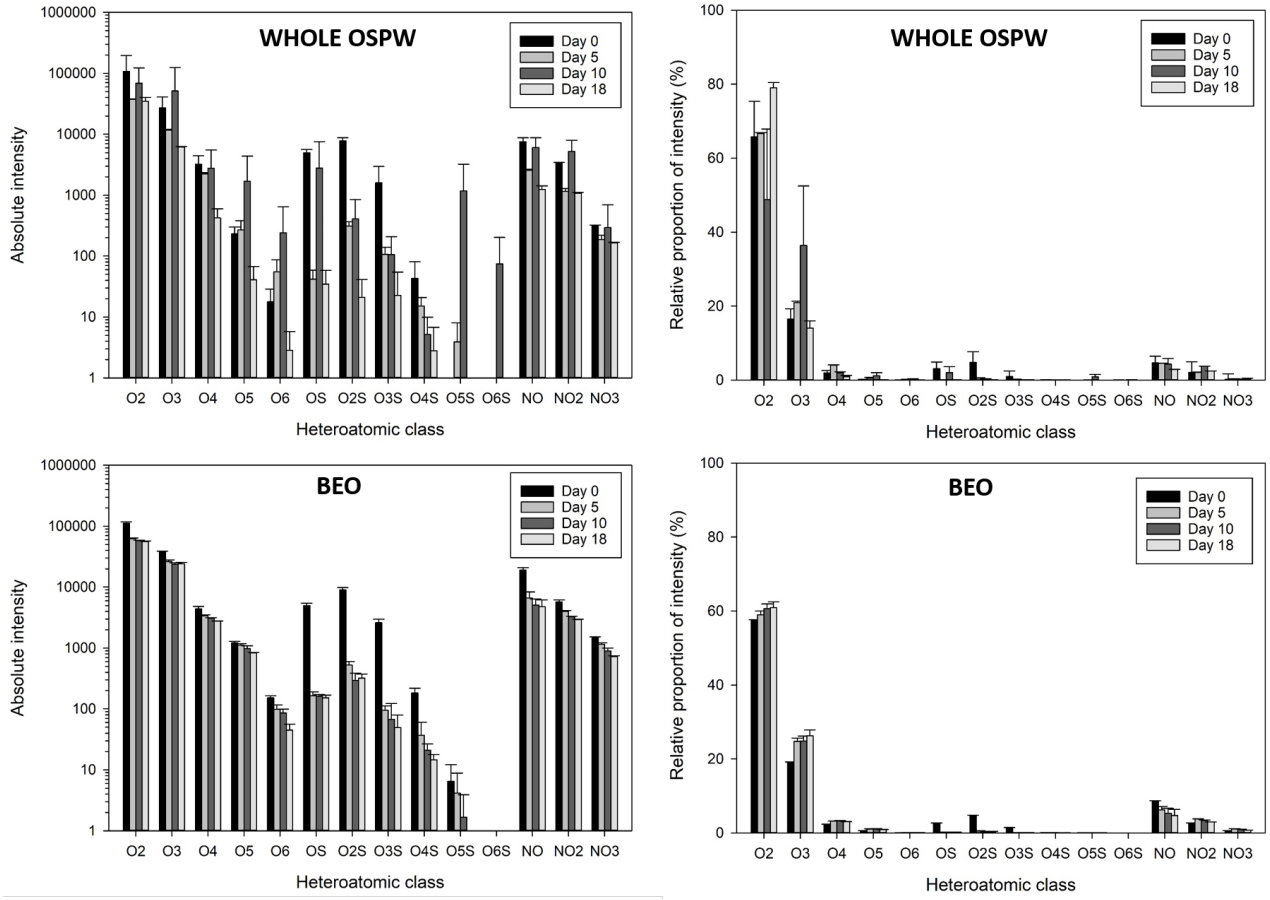

Figure 3 Mean (±SD) positive mode intensity by heteroatomic chemical class as absolute intensity (left) and relative proportion of total sample intensity (right) on days 0, 5, 10, and 18 of irradiation in whole OSPW (top) and base-extractable organic (BEO) samples (bottom) (n=3). All sample intensities are blank-subtracted.

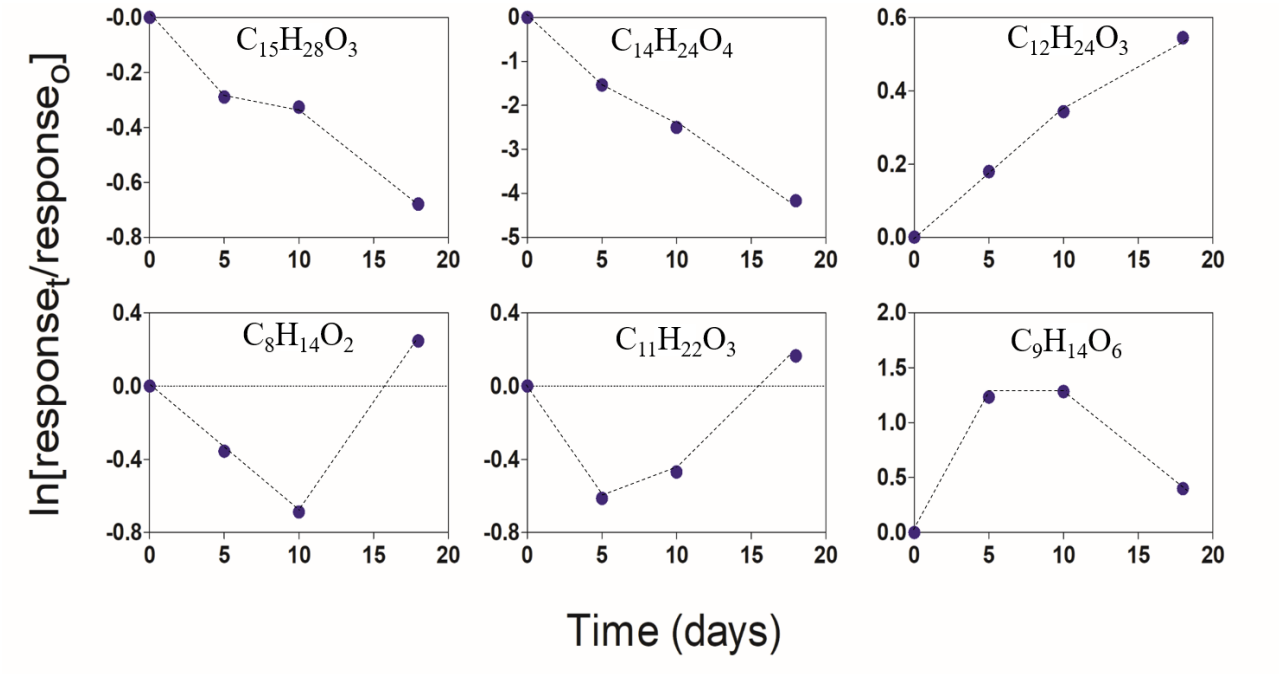

Figure 4: First-order kinetic time series plots for select species in whole OSPW samples analyzed in negative mode over 18 days of irradiation. Individual species were chosen to demonstrate the different kinetic behaviours observed among all species. The top panels show species following linear first-order decay or production, whereas the bottom panels highlight species demonstrating biphasic degradation and production kinetics over the 18 d experiment.

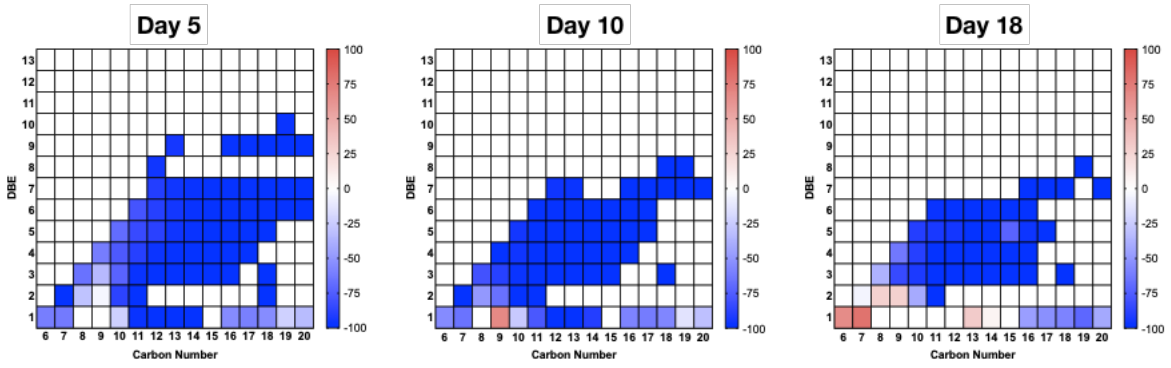

Figure 5: Heat maps of percent change relative to Day 0 for O_2^- species in whole OSPW after 5, 10, and 18 days or irradiation.

Tables

Table 1: Photolysis half-lives of individual heteroatomic chemical classes in OSPW from laboratory experiments and extrapolated to natural sunlight based on data from Lu et al. (2015). Spring, summer, and fall estimations apply to near surface processes only and are based on solar irradiance data at 50°N latitude on clear days. Mesocosm half-lives were estimated using sunlight intensity conditions at depth (8 cm) in outdoor mesocosms to account for light screening effects. These light intensity conditions were extrapolated from previous photolysis experiment conducted at the Prairie Wetland Research Facility at the University of Manitoba, Winnipeg, MB, Canada (49.9°N) in July, 2014 (Lu et al., 2015). Sunlight half-lives were only estimated for $OSPW^-$ samples to keep the table size manageable. †Halflives calculated from positive mode data.

Heteroatomic Class	Laboratory Values								Sunlight Extrapolation			
	OSPW (Positive Mode)				OSPW (Negative Mode)				OSPW ($t_{1/2}$ - d) (Negative Mode)			
	R^2	n	Slope	$t_{1/2}$ (d)	R^2	n	Slope	$t_{1/2}$ (d)	Spring	Summer	Fall	Mesocosm
O_2	0.58	68	-0.11	10	0.61	25	-0.10	11	234	146	461	717
O_3	0.59	71	-0.10	8	0.63	63	-0.12	15	311	195	613	953
O_4	0.71	47	-0.09	8	0.76	56	-0.23	6	131	82	258	402
O_5	0.55	22	-0.04	21	0.75	41	-0.14	7	153	95	301	468
O_6	n/a	n/a	n/a	n/a	0.71	25	-0.12	14	284	178	560	871
OS	0.51	5	-0.22	5	0.83	2	0.00	7	152	95	300	467
O_2S	0.78	14	-0.19	4	0.60	3	-0.09	9	194	121	381	593
O_3S	0.74	6	-0.14	4	0.50	9	-0.07	11	240	150	473	736
O_4S	0.82	2	-0.10	9	0.87	7	-0.31	3	57	36	112	174
ON	0.57	30	-0.08	8	n/a	n/a	n/a	n/a	168†	105†	330†	513†
O_2N	0.15	25	-0.04	18	n/a	n/a	n/a	n/a	377†	236†	742†	1155†
O_3N	0.41	20	-0.03	26	n/a	n/a	n/a	n/a	545†	340†	1072†	1668†
Average				**11**				**10**	**237**	**148**	**467**	**726**